International Conference on Space Optics—ICSO 2014

La Caleta, Tenerife, Canary Islands

7–10 October 2014

Compact tunable and reconfigurable microwave photonic filter for satellite payloads

M. C. Santos

O. Yoosefi

COMPACT TUNABLE AND RECONFIGURABLE MICROWAVE PHOTONIC FILTER FOR SATELLITE PAYLOADS

M. C. Santos and O. Yoosefi

Universitat Politècnica de Catalunya, Barcelona Tech
Jordi Girona 1, Campus Nord UPC-D3, 08034 Barcelona, Spain.
santos@tsc.upc.edu

I.   INTRODUCTION

The trend towards the photonic processing of electrical signals at microwave frequencies for satellite payloads is increasing at a breathtaking pace, mainly spurred by prospects of wide electrical bandwidth operation, low mass and volume, reduced electrical noise levels, immunity to electromagnetic interferences and resistance to both temperature and radiation [1-2].

Among the microwave signal processing functions required on-board satellites, spectral band selection and filtering is particularly challenging, especially for telecom applications where quite often a very narrow electrical passband is required and where tunability and reconfigurability are highly appreciated. A number of approaches for the design of filters at microwave frequencies based on photonic technologies, i. e. microwave photonic filters (MPF), has emerged showing tremendous potential in a variety of applications. In MPF the input RF signal is modulated over an optical carrier, processed in the optical domain, and then photodetected to provide the filtered RF output. Very comprehensive reviews of the topic of microwave photonic filtering may be found in [3-4].

A first subclass of MPF is based on discrete-time signal processing [5] which may in turn be broadly subdivided into the Finite Impulse Response (FIR) and the Infinite Impulse Response (IIR) types of MPF. FIR filters combine at their output a finite set of delayed and weighted replicas, or taps, of the input optical signal, while IIR filters are based on recirculating cavities to provide an infinite number of such replicas of the input optical signal. In order to ensure robustness against environmental changes, the overall majority of the proposed schemes work under the incoherent regime, i. e. the optical delays are much greater than the coherence time of the optical source. A fundamental drawback of incoherent approaches is related to Phase Induced Intensity noise (PIIN) due to the incoherent sum of signals. This is generally the dominant source of noise and it scales with the square of the signal power, just as the signal does, and therefore there are no simple ways of mitigating its effect [4]. It is also important to note that the spectral response of discrete-time MPFs is inherently periodic, where the Free Spectral Range (FSR) is inversely proportional to the tap delay, and usually presents a baseband response.

Direct synthesis MPF on the other hand, which rely on smart combinations of RF modulation of the optical carrier and optical filtering, are capable of providing a single passband response, are free from PIIN and feature very simple setups. As being free from the bias-drift problem, strategies based on phase rather than amplitude modulation are preferred. A typical example of Direct-synthesis MPF with phase modulation is found in [6], where use is made of two narrow band Fiber Bragg Gratings (FBG) with passbands tuned so that while one of them selects the optical carrier, their relative spectral distance gives the center frequency of the MPF. A 10 GHz MPF with   1 GHz bandwidth was reported [6]. A tunable center frequency MPF from 18 to 40 GHz with adjustable bandwidth from 5 to 15 GHz has been demonstrated based on this arrangement by using temperature tuned silicoñ on insulator microrings as passband optical filters [7]. A similar approach employs a notch optical filter to cancel one of the optical phase modulation sidebands out [8-9]. A narrow-band center frequency tunable MPF from 1 to 6.5 GHz with bandwidth on the 100 MHz range has been measured using a phase shifted FBG as the notch filter [9], but in such a setup the MPF bandwidth is fixed and determined by the optical filter bandwidth. In [10] the frequency detuning of the optical carrier with respect to the optical filter center frequency determines the bandwidth of the MPF, while the MPF center frequency is equal to the semi-bandwidth of the optical filter. Using temperature controlled FBGs and tunable lasers, center frequency tunable MPFs from 8 to 15 GHz with reconfigurable bandwidths on the GHz range have been reported [10].

We present a novel approach for the photonic filtering of microwave signals based on a direct-synthesis technique with optical phase modulation of the microwave signal and employing two tunable laser sources and a fixed optical passband filter. Both center frequency and bandwidth of the MPF may be controlled independently by proper selection of the respective laser wavelength detunings with respect to the filter cutoffs and therefore wide bandwidth fixed optical filters may be employed irrespective of the required MPF center frequency and

bandwidth. That allows to exploit the advantages of telecom-grade equipment, designed for fiber optic communications, with a high degree of maturity and very competitive prices. Owing to its direct-synthesis nature, the proposed MPF enjoys the advantages of single passband response and reduced noise levels, in a simple and compact setup. Experimental measures are provided using off-the-shelf fiber optic communications devices to support the feasibility of the method, along with simulated results based on Virtual Photonics Inc. (VPI), that show its potential.

The paper is structured as follows. We start with a description of the basic MPF setup and its principle of operation in section II. Next, the simulation procedures followed along with the results obtained are shown and analyzed in section III. In section IV we present the experimental setup and the measurements made and finally section V summarizes the main conclusions derived from the work.

II.   PRINCIPLE OF OPERATION

The basic scheme of the proposed direct-synthesis MPF is depicted in Fig. 1. It comprises two tunable laser sources with wavelengths lying within the passband of an optical filter and which may be adjusted to specific detunings with respect to the optical filter cutoffs. As seen, the laser outputs are coupled and fed to a single phase modulator (PM) which imprints the microwave input signal on both carrier wavelengths. After the modulator, the two phase modulated signals are optically filtered and then photodetected to provide the microwave output signal. Since this photodetector is only sensitive to optical envelope fluctuations, no microwave power is obtained whenever the whole double-sideband spectrum of the two optical phase modulated signals is comprised within the optical filter passband.

The microwave passband filtering effect of the described setup is understood as follows. Each of the optical carriers (f_2, f_1 , with $f_2 < f_1$) is placed respectively close to each of the cutoff wavelengths of the wideband optical filter (f_{c2}, f_{c1} , with $f_{c2} < f_{c1}$) so that their respective detunings respect to the closest cutoff are different ($\Delta f_1 = f_{c1} - f_1 \neq \Delta f_2 = f_2 - f_{c2}$), and their spectral difference $f_1 - f_2$ is so large that photomixing products among different laser output components fall outside the electrical band of interest. See the sketch in Fig. 1 for reference. The MPF passband frequency cutoffs will be given by $f_{ec1} = \min(\Delta f_1, \Delta f_2)$, $f_{ec2} = \max(\Delta f_1, \Delta f_2)$, as explained next and sketched in Fig. 2. For frequencies $f < f_{ec1}$ the whole spectrum of both phase modulated double-sideband optical signals is within the optical passband, and therefore there is no detected microwave signal at the photodiode output. Instead, for $f_{ec1} < f < f_{ec2}$, one of the sidebands of one of the two optical signals is filtered out yielding envelope fluctuations which provide a microwave power after photodetection. For $f > f_{ec2}$, both optical signals lose one of their sidebands, and have a different sign for their remaining sideband. The sidebands photomixing with the respective optical carriers yields opposite sign RF amplitude fluctuations which interfere destructively so that if the laser amplitudes and the optical filter insertion loss are adjusted to provide the same detected amplitudes, very low microwave power levels are obtained for $f > f_{ec2}$.
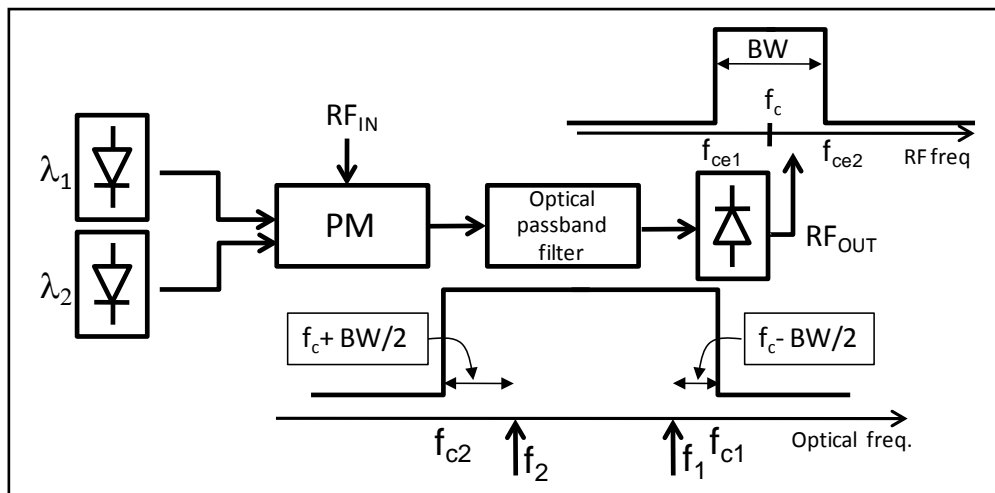
Fig. 1. Schematic of proposed MPF setup
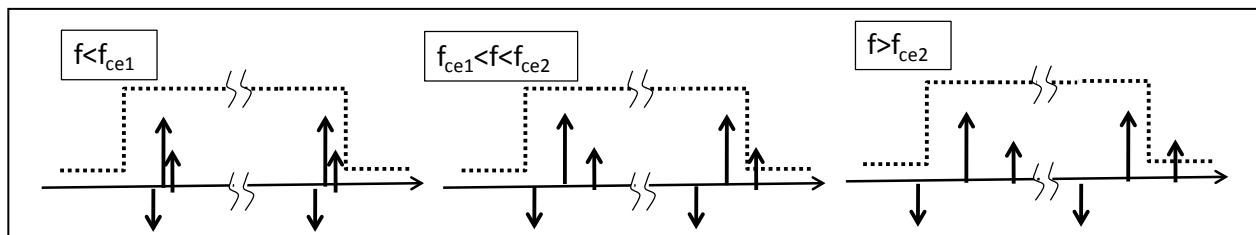
Fig. 2. Sketch of optical spectrum of PM output relative to optical filter spectral transfer function for different electrical frequency margins.

III. SIMULATION RESULTS

Fig. 3 shows the block diagram of the simulated system in VPI. The output power level and linewidth in both lasers is respectively 1 mW and 10 MHz. In the simulations the effect of uncorrelated phase noise has been accounted for by setting different random number seeds for the phase noise generation [11].

The use of a very low modulation amplitude value in the RF pure sine electrical wave generator ensures a narrow optical phase modulation spectrum which is expected to provide better results with the proposed method. In our simulations we have set a safety value of $0.1V_\pi$, with V_π the required voltage in the PM for a 180º optical phase shift, but we have checked out that slightly higher values are also appropriate.

The optical filter is a key element in the MPF setup. As explained, very wide bandwidths and moderately sharp cutoffs are advised. From the many options available in VPI for the optical filter we have selected an idealized trapezoidal transfer function with the minimum phase option active [11], so that the resulting filter is causal and hence physically realizable. Passband is set at 500 GHz around the center frequency and stopband attenuation at 506 GHz bandwidth is 30 dB. As shown in Fig. 3, a 2 port Analyzer has been connected to the photodiode output with the purpose of recording the photodetected amplitude values at the electrical frequency injected in the system by the electrical sine wave generator. In order to obtain the electrical spectral insertion loss transfer function of such an arrangement, automatic sweeps of the electrical frequency from 200 MHz to 40 GHz in 200 MHz steps have been run. The outcome of a series of simulations considering different values of the two input wavelengths is displayed in Fig. 4.

Fig. 4 a) shows the results of a variety of input wavelength combinations, all providing 1 GHz bandwidth, and center frequency passband values ranging from 2.5 GHz to 35.5 GHz. The insertion loss spectral transfer curves have been normalized to 0 dB but in all cases passband insertion loss were around 10 dB for the 1 mW power level lasers. The passband insertion loss in any case, scales with the lasers output power level so that even net gain can be obtained in the MPF passband for laser output power levels greater than 10 mW. Remarkable passband flat-top responses are observed which are maintained nearly unaltered throughout the broad tunability range. Fairly symmetrical bandpass-bandstop transitions are seen for moderate values of the passband center frequency (8.5 GHz, 12.5 GHz), but while in the lower frequency stopband the attenuation increases monotonically as the frequency is reduced, in the higher frequency stopband an insertion loss floor is reached at around 12 dB stopband attenuation for a 12.5 GHz center frequency passband. This insertion loss floor is seen to drop as the center frequency passband is increased, to reach a maximum stopband attenuation of 15dB at 35.5 GHz, and it rises up to a stopband attenuation of only 5 dB for 2.5 GHz center frequency passband. The contrast found between the shapes of the bandstop-passband transitions at the lower and the upper MPF cutoffs is a reflection of the different nature of the filtering mechanisms that take place at each MPF frequency cutoff. While in the lower frequency cutoff the transition from stopband to passband is due to the phase to amplitude conversion that comes from cancellation of one of the sidebands of one of the two phase modulated signals; the upper frequency cutoff occurs because of the destructive interference between the amplitudes detected when both phase modulated signals lose one of their sidebands to optical filtering.

Fig. 4 b) shows the capability for selecting a specific bandpass bandwidth of the proposed structure. A similar behaviour is observed with respect to the higher stopband insertion loss floor, i. e. it is seen to rise as the bandpass bandwidth is increased.
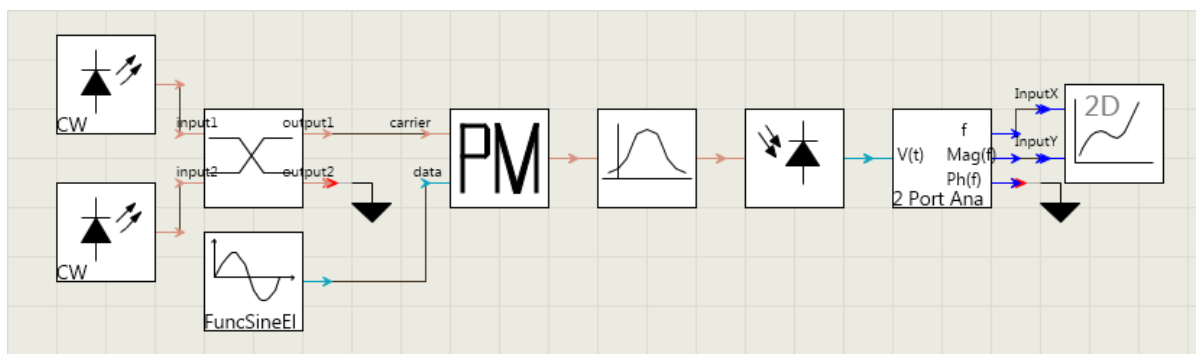
Fig. 3. VPI simulation setup.
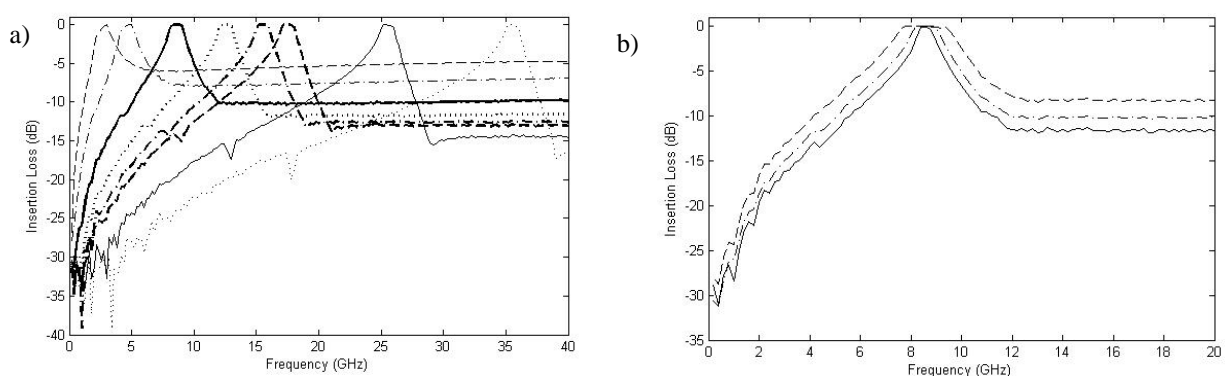
Fig. 4. MPF spectral transfer functions for different laser wavelength detunings (Δf_1, Δf_2) from the optical filter center frequency passband. a) dashed thin line: Δf_1=248 GHz, Δf_2= -247 GHz; dash-dot thin line: Δf_1=246 GHz, Δf_2= -245 GHz; solid thick line: Δf_1=242 GHz, Δf_2= -241 GHz; dotted thick line: Δf_1=238 GHz, Δf_2= -247 GHz; dash-dot thick line Δf_1=235 GHz, Δf_2= -234 GHz; dashed thick line: Δf_1=233 GHz, Δf_2= -232 GHz; solid thin line: Δf_1=225 GHz, Δf_2= -224 GHz; dotted thin line: Δf_1=215 GHz, Δf_2= -214 GHz. b) solid line: Δf_1=241.75 GHz, Δf_2= -241.25 GHz; dash-dot line: Δf_1=242 GHz, Δf_2= -241 GHz; dashed line: Δf_1=242.5 GHz, Δf_2= -240.5 GHz.

IV. EXPERIMENTAL RESULTS

In order to show the practical feasibility of the proposed MPF scheme, an experimental setup was assembled with off-the-shelf optical components, see Fig. 5. It consists of two diode laser sources: a Nortel Networks LC155W-20A Distributed Feedback (DFB) laser module in 14-pin butterfly package with ILX Lightwave LDC-3724B current and temperature controller, and a New-Focus 6427C external cavity laser (ECL). The broad tunability range of the ECL has been advantageously used in our experiments, but in practice telecom-grade temperature-tuned DFBs may be employed which can be found in the market at very competitive prices. As the phase modulating device, an integrated travelling-wave electro-optical lithium Niobate (LiNbO$_3$) phase modulator (PM) from Covega-Thorlabs, with 35 GHz RF bandwidth and V$_\pi$=5.5 V. has been used. As a consequence of the intrinsic anisotropy of the LiNbO$_3$ crystal, the modulation efficiency in the PM is dependent upon the direction of polarization of the input optical wave and it is maximum when both the optical and the electrical co-propagating waves follow the direction of the optical axis in the uniaxial LiNbO$_3$ crystal [12]. The phase modulator used in the experiment incorporates a polarization maintaining input optical fiber whose axis is oriented along the direction of maximum modulation efficiency, i. e. lower V$_\pi$. One polarization controller (PC) at the output of each laser serves the purpose of ensuring that the optical signals that arrive at the PM are aligned with the input fiber axis. A passive 50/50 optical coupler joins together the signals coming from each laser and transfers them to the input of the PM. After getting the phase modulation inside the PM, the two signals pass through the optical filter (OF), which is a 200 GHz bandwidth wavelength division multiplexing (WDM) channel selector with nominal center wavelength at 1547.72 nm corresponding to WDM channel 37. The output of the optical filter goes directly to an Agilent 83440D optical photodetector (PD) with 32 GHz bandwidth. An Agilent Vectorial Network Analyzer (VNA) N5245A provides the RF MPF input by connecting to the PM

electrical contact and retrieves the MPF output from the PD to yield swept frequency S21 insertion loss measurements, from 10 MHz to 50 MHz.

 The whole setup was laid on an optical table and proved to be very sensitive to the power levels used in the lasers and the VNA. By careful adjustment of all the parameters, we managed to get a filtering response which peaked at 15 GHz, as shown in Fig. 6, by setting the laser powers to 0dBm, the RF output to 10 dBm and the laser wavelengths to λ_1=1547.10 nm, λ_2=1548.28 nm.
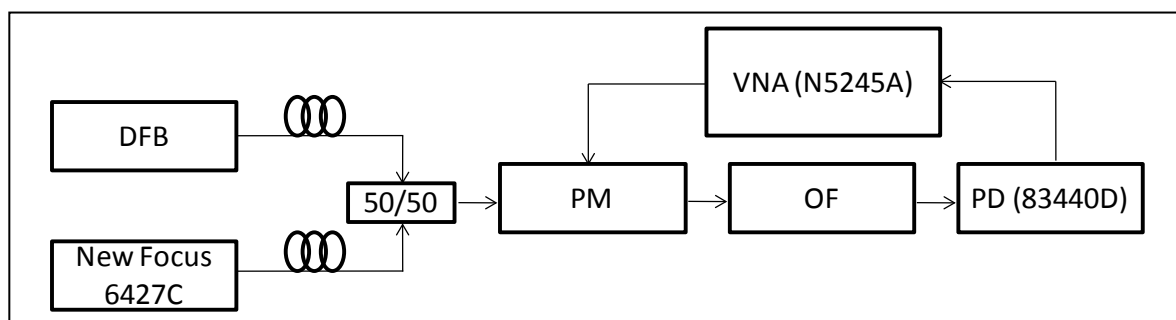
Fig. 5. Experimental setup.
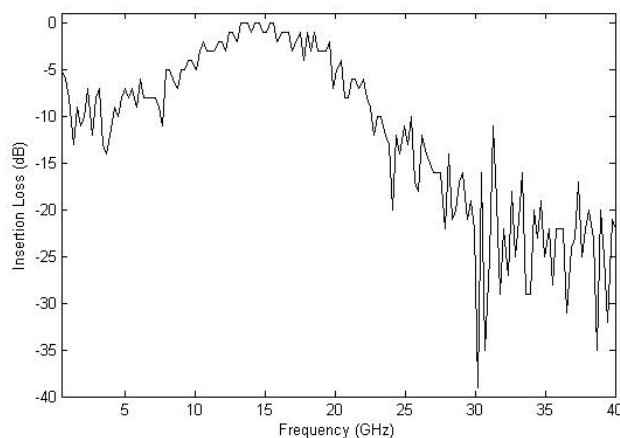
Fig. 6. Measured MPF spectral transfer function with λ_1=1547.10 nm, λ_2=1548.28 nm.

V. CONCLUSIONS

A novel scheme for the passband photonic filtering of signals in the microwave frequency range has been presented featuring both center frequency tunability and bandwidth adjustability. The microwave photonic filter proposed is simply reconfigured by control of the output wavelengths of two laser sources and relies on a direct-synthesis approach based on microwave optical phase modulation and optical filtering and thus it possesses a single-passband response and is free from phase induced interference noise. It is also expected to lead to robust and compact setups which may exploit the maturity of fiber optic equipment developed for the telecom industry, holding promise for satellite applications. Experimental results proving the RF filtering capability of the structure and using off-the-shelf equipment have been reported with a peak response at 15 GHz, and simulations have shown potential for broad center frequency tunability and bandwidth reconfigurability ranges. The conducted research has revealed the key role played by both the optical filter spectral transfer characteristic and the input power levels, both in the optical as well as in the electrical domain, and work is presently under way in order to improve the stability of the setup and to identify optical filtering structures that could help to optimize the MPF characteristics.

REFERENCES

[1] A. Bensoussan and M. Vanzi, "Optoelectronic devices product assurance guideline for space application," in Proceedings of ICSO 2010: International Conference on Space Optics (ESA, 2010), pp. 8–13.

[2] M. Sotom, B. Benazet, A. Le Kernec, and M. Maignan,"Microwave photonic technologies for flexible satellite telecom payloads," in Proceedings of the 35th European Conference on Optical Communication, 2009 (IEEE, 2009), pp. 20–24.

[3] J. Capmany, J. Mora, I. Gasulla, J. Sancho, J. Lloret and S. Sales,"Microwave Photonic Signal Processing", J. of Lightw. Technol. vol. 13, no. 4, Feb 2013.

[4] R. A. Minasian, "Photonic Signal Processing of Microwave Signals", IEEE Trans. Microw. Theory Tech., vol. 54, no. 2, Feb 2006.

[5] J. Capmany, B. Ortega, D. Pastor, and S. Sales, "Discrete-time optical processing of microwave signals," J. Lightw. Technol., vol. 23, no. 2, pp. 702–723, Feb. 2005

[6] X. Yi and R. A. Minasian, "Microwave Photonic Filter with single-bandpass response", Electron. Lett.,vol. 45, No. 7, March 2009. .

[7] D. Zhang, X. Feng and Y. Duang, " Tunable and Reconfigurable Bandpass Microwave Photonic Filters Utilizing Integrated Optical Processor on Silicon-on-Insulator Substrate", IEEE Photon. Technol. Lett., vol. 24, No. 17, Sept 2012.

[8] J. Palací, G.E. Villanueva, J. V. Galan, J. Marti and B. Vidal, IEEE Photon. Technol. Lett. Vol. 22, pp. 1276 (2010).

[9] W. Li, M. Li and J. Yao, " A Narrow-Passband and Frequency-Tunable Microwave Photonic Filter Based on Phase-Modulation to Intensity-Modulation Conversion Using a Phase-Shifted Fiber Bragg Grating", IEEE Trans. Microwave Th. And Tech., Vol 60, No. 5, May 2012.

[10] T. Chen ,X. Yi, L. Li and R. Minasian, "Single passband microwave photonic filter with wideband tunability and adjustable bandwidth", Optics Letters Vol. 37,No 22,pp 4699-4701, Nov 2012.

[11] VPI transmission maker, photonic modules reference manual. Virtual Photonics Systems Inc. 2002.

[12] B. E. A. Saleh and M. C. Teich, "Fundamentals of Photonics", 2nd Edition, John Wiley & Sons, 2007.